INVESTIGATING THE IMPACT OF DEFORESTATION ON MICROCLIMATE AND INCREASING THE RISK OF HEAT STRESS USING SATELLITE IMAGE PROCESSING (CASE STUDY: FORESTS OF HIRAN AREA)

J. Jafarzadeh [1]*, A.A. Kakroodi[2], Y. Erfanifard[3]

[1] PhD candidate, Geography Faculty, University of Tehran, Tehran, I.R. Iran – jafar.jafarzadeh@ut.ac.ir
[2] Geography Faculty, University of Tehran, Tehran, I.R. Iran – a.a.kakroodi@ut.ac.ir
[3] Geography Faculty, University of Tehran, Tehran, I.R. Iran – erfanifard@ut.ac.ir

Commission IV, WG IV/3

KEY WORDS: Deforestation, Land Surface Temperature, Microclimate, Heat Stress, Satellite Image, Landsat

ABSTRACT:

In recent years, the forests of northern Iran, which have a very high value, have been changed and turned into other uses due to various human reasons. Meanwhile, residential and road construction is more visible in these forests. Recognizing the location and investigating the impact of changes in forest extent in any region can greatly help the condition of forests in the past and planning their restoration. In this research, using satellite image processing, the effect of deforestation on the microclimate of the region and its effect on the surface temperature of the region have been investigated. By collecting in situ points in sixty samples including thirty tree areas and thirty pasture and treeless areas, the forest rate was determined using the normalized vegetation cover index. Then the land surface temperature of the studied area was calculated using the single channel method. Finally, by choosing a region as a control region in order to control the impact of global warming, the studied region and the control region were statistically compared. The results of the classification of the region based on tree and non-tree areas showed that during the years 1984 to 2021, about 1400 hectares were deforested. Also, the results of the final Welch T_test statistical test showed that there is a significant difference between the temperatures of the two regions at the 99% confidence level and with a p_value equal to 0.0007. This fact shows the significant impact of deforestation on increasing the temperature of the region.

1. INTRODUCTION

1.1 Theoretical Foundations

A forest is a vast area covered with trees, shrubs and other animals that share life together and is an important part of the earth's ecosystem, which has the main task of absorbing carbon dioxide and producing oxygen in the photosynthesis cycle, to maintain the environmental balance (Ya'acob et al., 2012). Meanwhile, deforestation is one of the main reasons for reducing biodiversity in the world and is the main source of carbon emissions (Higginbottom et al., 2019). It also causes climate changes, habitat loss and other devastating effects (Kim, 2010). Deforestation has been recognized as one of the biggest global environmental problems (Bruvoll et al., 2003; Dobson et al., 1997; Sodhi et al., 2004). Deforestation is one of the main components of land use changes and has been recorded as the biggest threat to global biodiversity (Sala et al., 2000). In recent decades, remote sensing data have been widely used to provide land use/land cover information such as the reduction of forest and swamps, urbanization rate and intensity of agricultural activities and other man-made changes (Alrababah and Alhamad, 2006). Satellite images have been widely used for classification processes, especially in the preparation of user or cover maps and the discovery of land cover conditions (Lobo et al., 2004). The forests of the north of Iran, which have a very high value, have been changed and turned into other uses in the past years and due to various reasons. Recognizing the location and determining the rate of changes in forest extent in any region can greatly help the condition of forests in the past and planning their restoration (Ghanbari and Shatai, 2019). Zheng et al. (2021) investigated the warming caused by deforestation in tropical mountainous regions that changes by altitude. In this research, they found that the local temperature anomaly caused by deforestation can reach up to 2 degrees Celsius, where the forest conversion is extensive. He et al. (2015) in research investigated the change in the amount of energy budget observed by satellite from deforestation in Northeast China and its climatic consequences. This study presents the potential change in energy budget due to deforestation in northeast China and its climate consequences, which is evaluated by quantifying the differences observed in MADIS images of surface physical characteristics between cropland and forest. De Frenne et al. (2021) reviewed forest microclimates and climate change: importance, drivers and future research agenda. In this research, they investigated how spatial and temporal changes in forest microclimates are caused by the mutual influence of forest characteristics, local water balance, topography and landscape composition. Hashemi et al. (2016) investigated the monitoring of forest cover changes in Siah Mezgi basin of Gilan province using Landsat images. The results showed that the area of forest land decreased by 213.55 hectares between 2000 and 2015.

In this research, it is tried to use the Landsat satellite image processing and calculate the surface temperature and also extract the density of trees in the study area in Hiran forests located on the border of Gilan and Ardabil provinces and also the border of the Republic of Azerbaijan using the normalized vegetation index, to investigate the relationship between deforestation and destruction of trees in the region with heat stress. The final results

* Corresponding author

will show the relationship between deforestation and temperature using statistical analysis and various statistical tests.

1.2 Materials and Methods

1.2.1 Study area

The area studied in this research is an area of 47,590 hectares located in the north of the Islamic Republic of Iran. This area is located in the two provinces of Gilan and Ardabil, as well as parts of the border of the Republic of Azerbaijan, and is considered one of the forest areas of Iran. These forests are among Hyrcanian forests. The studied area extends from 48.33 degrees to 48.50 degrees east longitude to 38.23- and 38.26-degrees north latitude. Iran's forests have a total of 3,400,000 hectares of forest on the northern slopes of the Alborz Mountains and the coastal provinces of the Caspian Sea. The area of other forests that are scattered in other parts of the country is up to three million hectares. Figure 1 shows the studied area.

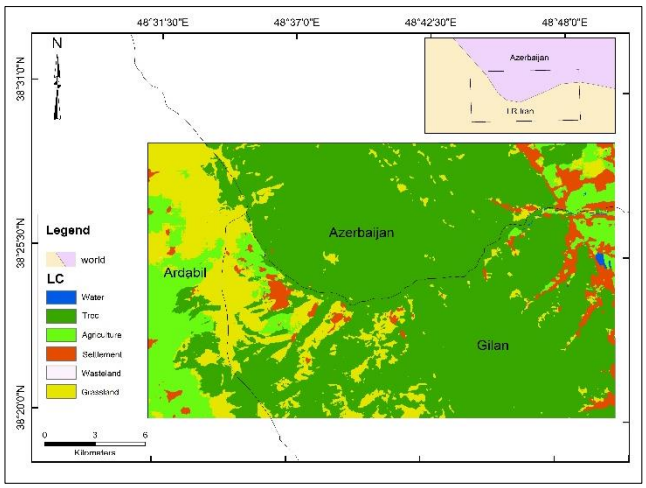

Figure 1. The study area.

1.2.2 Data used

In this research, the data of Landsat 4, 5 and 8 related to the years 1984, 1994, 2005, 2014 and 2021 have been used(appendix1). Also, the classified image of land use related to Sentinel 2 satellite has been used to introduce the studied area. ArcGIS software version 8.10 and satellite image processing software ENVI version 5.3 are used in this research. Also, RStudio programming software was used for the statistical analysis of this research.

1.3 Research Methods

1.3.1 Normalized Differential Vegetation Index (NDVI)

The Normalized Difference Vegetation Index (NDVI) is a simple graphical index that is used in remote sensing analysis and measurements to assess the presence or absence of vegetation in an area. The range of changes of this index is between +1 and -1. This index is calculated through equation 1 (Gates, 1980):

$$NDVI = \frac{(NIR-RED)}{(NIR+RED} \quad (1)$$

Where NIR=Near Infra-Red Band
RED= Red Band

1.3.2 Calculation of LST

Any object that has a temperature higher than zero degrees Kelvin emits thermal radiation and this energy is emitted from objects or the surface of the earth (Alavi-Panah, 2008).

Single channel method

In the single-channel method, LST is calculated through equation (2) (Isaya and Avdan, 2016):

$$T_s = \gamma[\varepsilon^{-1}(\psi_1 \times L_{sensor} + \psi_2) + \psi_3] + \delta \quad (2)$$

Where Ts=LST
T_{sensor} = sensor brightness temperature in Kelvin
γ= effective wavelength of a thermal infrared band
ψ= atmospheric effect modifier on
L_{sensor}=thermal radiance

To calculate the amount of γ, we use equation number 3 (Cristóbal et al. 2018):

$$\gamma = \left\{\frac{C_2 L_{sensor,\lambda}}{T^2_{sensor}}\left[\frac{\lambda^4}{C_1} L_{sensor,\lambda} + \lambda^{-1}\right]\right\}^{-1} \quad (3)$$

Where C1 and C2 = coefficients of atmospheric parameters
λ= wavelength.

Shapiro-Wilk test

The Shapiro-Wilk test is one of the normal distribution fitting tests. With the help of this test and its statistic, you can determine whether the data follows a normal distribution or not. According to this issue, this test can be considered as part of the group of non-parametric statistics methods (Beyer, 2002). In order to determine whether or not to reject the null hypothesis, we rely on the probability value (P-value) that is produced in most statistical software. If the value of Sig is less than 0.05, we reject the null hypothesis and conclude that the sample data were not extracted from a normal population (Vogt, 2005). Equation 4 shows the test statistic:

$$W = \frac{\left(\sum_{i=1}^{n} a_i x_{(i)}\right)^2}{\sum_{i=1}^{n}(x_i - \bar{x})^2} \quad (4)$$

$\bar{x}$ means the mean of observed values from a random sample.

t-test with two independent samples

This test compares the average of two groups of respondents. In other words, in this test, the averages obtained from random samples are judged. This means that we randomly select samples from two different communities, regardless of whether the number of samples is equal or unequal, and compare the averages of those two communities. (Mansour Far, 2014).

T-welch test

This test, like the two-sample T-test, is used to compare the average of two populations. In Welch's T-test, it is assumed that the variance of two populations is not equal (Welch, 1947).

2. RESULTS AND DISCUSSION

By referring to the study area and using a single-frequency handheld GPS device model Garmin 12, land points were taken from the study area. These points are 60 points related to the area with tree cover and the areas with pasture and grass vegetation. Sampling was done randomly and included 30 points related to the areas with tree cover and 30 points from the vegetation areas of pasture and grass, which, in compliance with the spatial resolution of the Landsat image, which is 30 meters, in the form of distances of less than thirty meters and more It was taken thirty meters from each other. The points related to the tree vegetation include the places where the tree cover is dense and has thick trees, as well as the areas that have low density trees and young trees. By calling the harvested points in ENVI software and

matching it with the studied area, the spectral reflectance values of the harvested points are checked and its difference with other points is checked. By examining this difference and determining a threshold value on the normalized vegetation index image, in the next step, the normalized vegetation index image was reclassified with new values in two classes. Threshold values were determined by examining the difference between the collected points on the ground and comparing it with the satellite image and the normalized vegetation index image. This threshold limit was determined experimentally and as the average value of 30 points taken. Figure 2 shows the calculated vegetation indices for the study area during the years 1984 to 2021 in the form of a ten-year time series. Figure 2 shows the calculated vegetation indices for the study area during the years 1984 to 2021 in the form of a ten-year time series. In order to avoid too much content, we have shown the vegetation index calculated for one year in Figure 2.

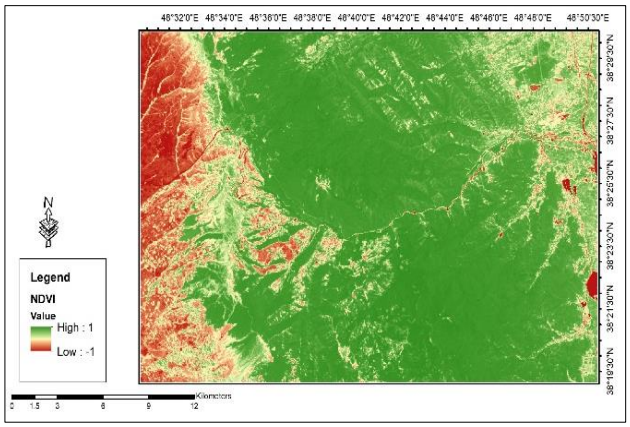

Figure 2. Vegetation indicators calculated for the study area in 2021.

Figure 3 shows the separation of the tree layer from the pasture and others based on the analysis of the spectral graph of the pixels and the correspondence with the ground control point for 2021.

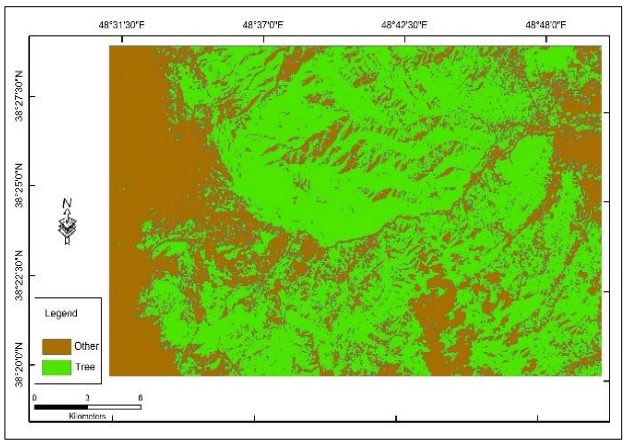

Figure 3. Separation of tree class from pasture and others for 2021 (as an example).

Table 1 and Figure 4 show the amount of forest changes in the study area from 1984 to 2021. As can be seen from the data in the table, the reduction of about 2000 hectares of trees in the study area during the years under study is observed, which is mainly due to the field visits, including the destruction for the construction of villas and housing, and also, as a result, the destruction to create a communication path for access. to these places. Table No. 1 and Figure No. 4 show the amount of forest changes in the study area from 1984 to 2021. As can be seen from the data in the table, the reduction of about 2000 hectares of trees in the study area during the years under study is observed, which is mainly due to the field visits, including the destruction for the construction of villas and housing, and also, as a result, the destruction to create a communication path for access. to these places.

Year	Value (Hectar)	Tree Density
1984	40266	0.861
1994	40020	0.840
2005	39761	0.835
2014	39102	0.821
2021	38850	0.816

Table 1. Changes of trees in the study area from 1984 to 2021.

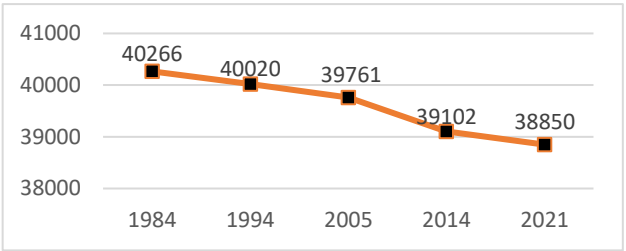

Figure 4. The diagram of forest changes from 1984 to 2021 in the study area (hectares).

Figure 5 shows the calculated temperature map for the study area for the year 2021 (as an example) in degrees Celsius. To convert degrees Kelvin to Celsius, just replace the calculated image with the expression b1-273.15.

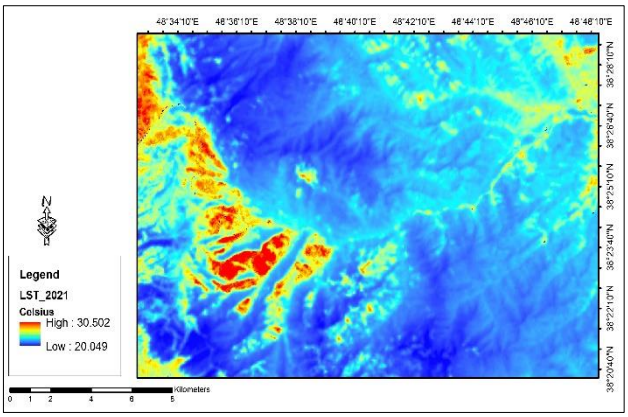

Figure 5. Land surface temperature in degrees Celsius.

Table No. 2 shows the average changes in the earth's surface temperature calculated for the years 1984 to 2021 in terms of Kelvin and degrees Celsius. Figure No. 6 is a diagram related to Table No. 2, which shows the average temperature changes. According to the calculated values, the amount of temperature changes between 1984 and 2021 for the studied area is equivalent to 0.85 degrees Celsius.

Year	Kelvin	Celsius
1984	295.315	22.165
1994	295.500	22.350
2005	296.711	22.561
2014	297.834	22.684
2021	297.162	23.012

Table 2. Calculated average temperature for the years 1984 to 2021 in Kelvin and degrees Celsius.

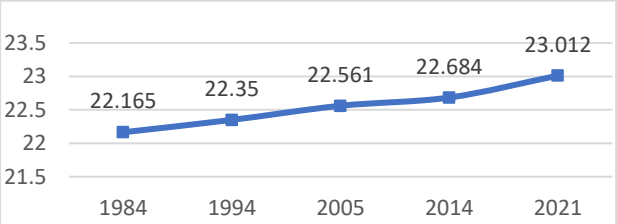

Figure 6. Temperature changes in the studied area in degrees Celsius.

In the continuation of the work, in order to be able to separate and model the temperature changes in the study area from the average global temperature changes, select an area close to the study area either with the same area or with an area equivalent to densitometry. we do. We consider the area we have worked and calculated its temperature as the treatment or test area and consider the new area as the control area so that we can model the process of changes in temperature and tree density. So, in the continuation of the work, we also calculate the average temperature changes of the surface of the new area. Figure 7 shows the location of the modelling control area with an area of one tenth of the studied area. The control area within the study area and in the part where almost no destruction (or at least very little destruction) has not taken place in the forest and cutting of trees has been chosen to show the amount of temperature changes during the studied years and the ratio between global changes. and find out an area.

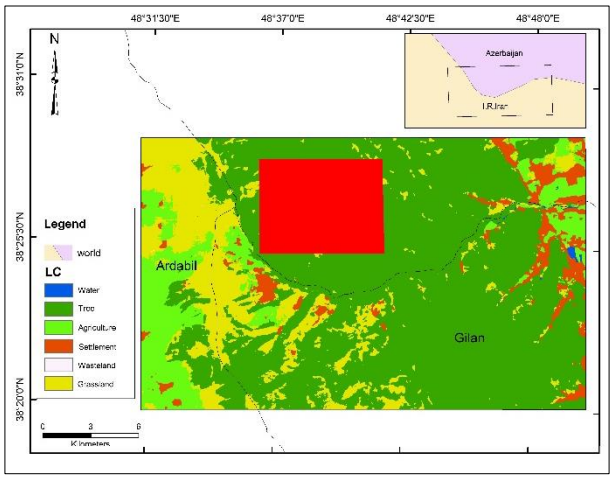

Figure 7. Control region for final modelling.

Table No. 3 shows the average surface temperature changes of the control area during the studied years. Also, figure number 8 of the chart related to table number 3 shows the average temperature changes of the control area in Celsius units. Figure 9 shows the temperature calculated for the control area in degrees Celsius for 2021 (as an example)

Year	Kelvin	Celsius
1984	294.314	21.164
1994	294.340	21.190
2005	294.342	21.192
2014	394.367	21.217
2021	294.372	21.222

Table 3. Calculated average temperature for the years 1984 to 2021 in Kelvin and degrees Celsius for the control area.

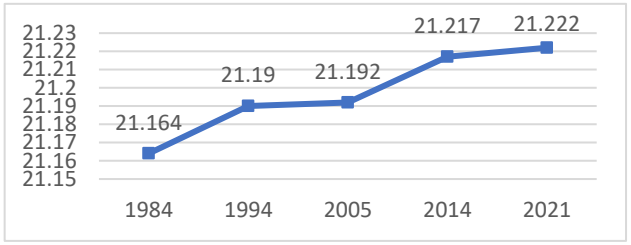

Figure 8. Temperature changes in the control area in degrees Celsius.

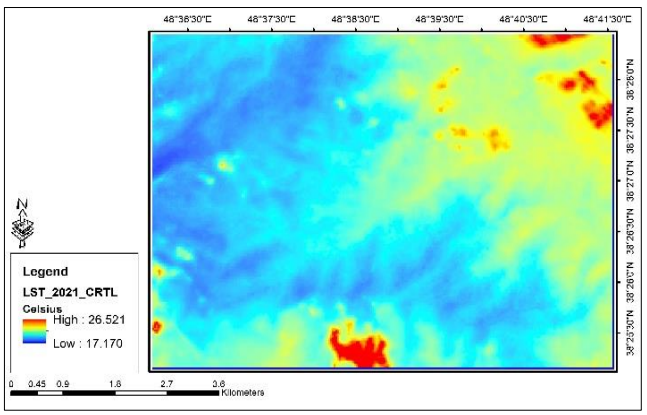

Figure 9. Calculated temperature for the control area in degrees Celsius for the year 2021.

The authors are aware that temperature increase is a global phenomenon and to control this disturbing variable, an area without deforestation and tree cutting was considered as a control group and compared with the studied area. Shapiro-Wilk statistical tests, independent t-test, Lune's test and Welch's independent t-test were used for statistical comparisons of two regions, and we will explain the results obtained from the implementation of these tests in RStudio programming software (appendix 2).

Table No. 4 and Figure No. 10 show the average temperature changes of the control area and the test area in terms of Kelvin and degrees Celsius during the years 1984 to 2021.

	Control Group		Experiment Group	
Year	Kelvin	Celsius	Kelvin	Celsius
1984	294.314	21.164	295.315	22.165
1994	294.340	21.190	295.500	22.350
2005	294.342	21.192	296.711	22.561
2014	294.376	21.217	294.834	22.648
2021	294.372	21.222	297.162	23.012

Table 4. The average temperature changes of the control area and the test area in terms of Kelvin and degrees Celsius during the years 1984 to 2021.

This contribution has been peer-reviewed. The double-blind peer-review was conducted on the basis of the full paper.
https://doi.org/10.5194/isprs-annals-X-4-W1-2022-315-2023 | © Author(s) 2023. CC BY 4.0 License.

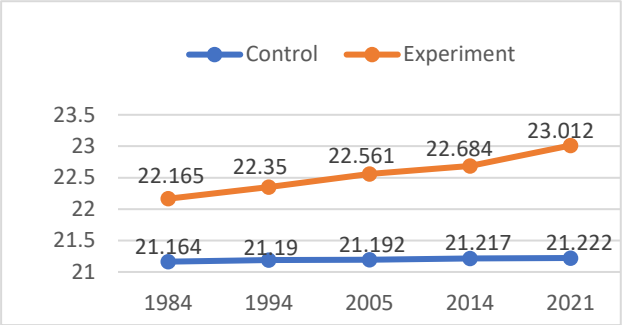

Figure 10. The average temperature changes of the control area and the test area in degrees Celsius during the years 1984 to 2021.

Shapiro-Wilk normality test			
Control Area		Experiment Area	
P-Value	0.5842	P-Value	0.968
w	0.92821	w	0.98695

Table 5. Shapiro-Wilk test results

The results of the Shapiro-Wilk test showed that the temperature data in degrees Celsius in the two control areas with a probability value of 0.5842 and the experimental area with a probability value of 0.968 had a normal distribution, which is shown in Table No. 5. Figure 11 shows the Q-Q plot to show the normality of the data. Also, for more intuition, the curve diagram of the empirical data distribution function is drawn on the theoretical normal distribution function in figure number 12.

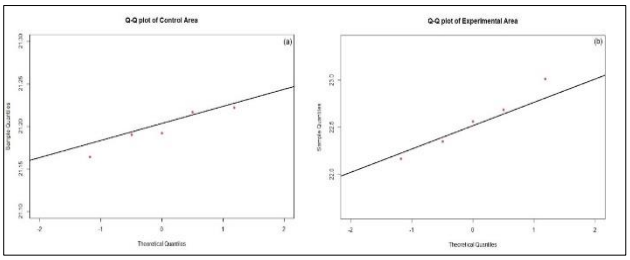

Figure 11. Q-Q plot to show the normality of the data of (a) control region and (b) test region.

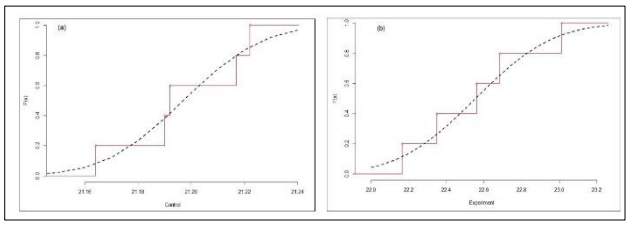

Figure 12. Experimental plot to show the normality of the data of (a) control area and (b) test area.

Since the data of both regions had a normal distribution according to the Shapiro-Wilk test, independent T-test can be used to check the equality of the average temperature of the two control and experimental regions. For this purpose, we first use Lon's test to check the equality of variances of two data groups. The results of Lon's test rejected the hypothesis of equality of variances at the 95% confidence level (P-value=0.03145). Therefore, due to the unequal variances of the two groups, we use the Welch T-test. This test rejected the hypothesis of equality of temperature between the two control areas and the test area at a very high significant level (99%) (P-value = 0.0006944).

3. CONCLUSION

Destruction of forest areas and in the term, deforestation has been one of the unfortunate consequences of human intervention on the planet. Meanwhile, in recent years, the forests of northern Iran, which have a very high value, have been transformed into villas and roads due to various human reasons. In this research, an attempt was made to investigate the effect of deforestation on the microclimate of the region and its effect on the surface temperature of the region by using the processing of Landsat satellite images during the period from 1984 to 2021 and in a ten-year time series. By collecting land points in sixty samples including thirty tree areas and thirty pasture and treeless areas, the forest rate was determined using the normalized vegetation cover index. Then the surface temperature of the studied area was calculated using the single channel method. Finally, by choosing a region as a control region in order to control the impact of global warming, the study region and the control region were statistically compared. The results of the classification of the region based on the areas with trees and non-trees showed that during the years 1984 to 2021, about 1416 hectares were deforested, which was reduced from 0.861 percent to 0.816 percent by calculating the density of trees in the region. it shows. Also, the calculation of the surface temperature of the area showed that the temperature of the studied area had an upward trend of about 0.847 degrees Celsius during this period of time. Finally, the results of the final Welch T_test showed that there is a significant difference between the temperatures of the two regions at the 99% confidence level and with a p_value equal to 0.0007. This fact indicates the significant effect of deforestation on the increase in temperature in the region, which by removing the disturbing variable of global temperature increase by choosing the control area, this probability value indicates the strong effect of deforestation on the increase in temperature stress in the studied area.

REFERENCES

Alavi-Panah, Seyyed Kazem. 2008: *Thermal remote sensing*. Tehran University Printing and Publishing Institute. Sixth edition. 666 p.

Alrababah, M.A. and Alhamad, M.N. 2006. Land use/cover classification of arid and semi-arid Mediterranean landscapes using Landsat ETM. *International Journal of Remote Sensing*, 27: 2703-2718.

Beyer, W. H. 2002: *CRC Standard Mathematical* Tables, 31st ed. Boca Raton, FL: CRC Press, pp. 536 and 571.

Bruvoll, A., Fahn, T. and Strom, B. 2003. Quantifying central hypotheses on Environmental Kuznets Curves for a rich economy: a computable general equilibrium study, *Scottish Journal of Political Economy*, 50(2): 149–173.

Cristóbal, J.; Jiménez-Muñoz, J.C.; Prakash, A.; Mattar, C.; Skoković, D.; Sobrino, J.A. An Improved Single-Channel Method to Retrieve Land Surface Temperature from the Landsat-8 Thermal Band. Remote Sens. 2018, 10, 431. https://doi.org/10.3390/rs10030431

De Frenne, P., Lenoir, J., Luoto, M., Scheffers, B. R., Zellweger, F., Aalto, J., … Hylander, K. 2021. Forest microclimates and climate change: Importance, drivers and future research agenda. *Global Change Biology*, 27(11), 2279–2297. doi:10.1111/gcb.15569

Dobson, A. P., Bradshaw, A. D. and Baker, A. J. M. 1997. Hopes for the future: restoration ecology and Conservation biology, Science, 227: 515- 522.

Ghanbari, F., and Shatai Juibari, Sh. 2009. Examining the process of forest level changes using aerial photos and ASTER images (case study: marginal forests in the south and southwest of Gorgan city). Wood and Forest Science and Technology Research, 17(4), 1-18.

Gates, David M. 1980: *Biophysical Ecology*, Springer-Verlag, New York, 611 p.

Hashemi, S., Fatemi Talab, S., Kavousi Kalashmi, H., Madanipour Kermanshahi, M. 2016. Change detection in the forest cover of Siyahmezgi watershed of Guilan using LandSat images. *Journal of RS and GIS for Natural Resources*, 7(3), 78-88.

He, T.; Shao, Q.; Cao, W.; Huang, L.; Liu, L. Satellite-Observed. 2015: *Energy Budget Change of Deforestation in Northeastern China and its Climate Implications*. Remote Sens. 7, 11586-11601. https://doi.org/10.3390/rs70911586

Higginbottom TP, Collar NJ, Symeonakis E, Marsden SJ. 2019. Deforestation dynamics in an endemic-rich mountain system: Conservation successes and challenges in West Java 1990–2015. *Biological Conservation*, 229: 152-159.

Isaya Ndossi, M.; Avdan, U. 2016. Application of Open-Source Coding Technologies in the Production of Land Surface Temperature (LST) Maps from Landsat: A PyQGIS Plugin. Remote Sens. 8, 413. https://doi.org/10.3390/rs8050413

Kim OS. 2010. An assessment of deforestation models for reducing emissions from deforestation and forest degradation (REDD). *Transactions in GIS*, 14(5): 631-654.

Lobo, A., Legendre, P., Rebollar, J.L.G., Carreras, J. and Ninot, J.M. 2004. Land cover classification at a regional scale in Iberia: Separability in a multitemporal and multi-spectral data set of satellite images. *International Journal of Remote Sensing*, 25: 1. 205-213.

Sala O. E., Chapin F. S. I., Armesto J. J., Berlow E., Bloomfield J., Dirzo R., Huber- Sanwald E., Huennu K. L. F., Jackson R. B., Kinzig A., Leemans R., Lodge D.M., Mooney H. A., Oesterheld M., Poff N. L., Sykes M. T., Walker B. H., Walker M., and Wall D. H. 2000. Global biodiversity Scenarios for the year 21000", Science, 287:1770- 1774.

Sodhi N. S., Pinkoh L., and Brook B. W. 2004 Southeast Asian biodiversity: an impending disaster, Trends in Ecology and Evolution, 19:654- 660

Vogt, W.P. 2005: *Dictionary of Statistics & Methodology: A Nontechnical Guide for the Social Sciences*. SAGE.

Welch, B. L.1947. "The generalization of "Student's" problem when several different population variances are involved". Biometrika. 34 (1–2): 28–35.

Ya'acob N, Azize ABM, Mahmon NA, Yusof AL, Azmi NF, Mustafa N. 2014. Temporal forest change detection and forest health assessment using Remote Sensing. In: IOP Conference Series: Earth and Environmental Science, vol 1. *IOP Publishing*, p 012017.

APPENDIX

1- Specifications of Landsat satellite images used in this research

Pass	Row	Date	Landsat Scene
167	033	1984/08/20	LT05_L1TP_167033_19840820_20170220_01_T1
167	033	1994/05/28	LT05_L1TP_167033_19940528_20180608_01_T1
167	033	2005/06/11	LT05_L1TP_167033_20050611_20200902_02_T1
167	033	2014/07/22	LC08_L1TP_167033_20140722_20170421_01_T1
167	033	2021/06/23	LC08_L1TP_167033_20210623_20210629_01_T1

2- Pseudocode related to the statistical analysis of research under RStudio software

```
rm(list=ls())
 library(readxl)
   Data <- read_excel("C:/Users/karbar/Desktop/data.xlsx")
   View(Data)
 Data1<-Data[1:5,]
 Data2<-Data[6:10,]
       shapiro.test(Data1$Celsius)## test of normality
       shapiro.test(Data2$Celsius)## test of normality
##
 library(car)
   leveneTest(Celsius ~ group, data = Data)
   t.test(Celsius ~ group1, data = Data)#independent T-test
##
 library(ggplot2)
    qplot(year,Celsius,data = Data,color=group)
#
     x<-Data1$Celsius
     y<-Data2$Celsius
        plot.stepfun(x, col=2,lwd=2,ylab="F(x)",xlab="x",main="")
     z1<-seq(21,21.5,.01)
     z2<-seq(22,23.3,.01)
#########
   plot.stepfun(x, col=2,lwd=2,ylab=paste("F(x)"),xlab="Control",main="",frame.plot=F)
        lines(z1,pnorm(z1,mean(x),sd(x)),lwd=2,col=1,lty=2)
   plot.stepfun(y, col=2,lwd=2,ylab=paste("F(x)"),xlab="Experiment",main="",frame.plot=F)
        lines(z2,pnorm(z2,mean(y),sd(y)),lwd=2,col=1,lty=2)
##
   qqnorm(x,main="Q-Q plot of Control Area",col=2,cex=1,pch=16,xlim=c(-2,2),ylim = c(21.1,21.3))
              qqline(x,col=1,lwd=2)
   qqnorm(y,main="Q-Q plot of Experimental Area",col=2,cex=1,pch=16,xlim=c(-2,2),ylim = c(21.6,23.4))
              qqline(y,col=1,lwd=2)
```